Environmental Science: Atmospheres

ROYAL SOCIETY OF CHEMISTRY

PAPER

View Article Online
View Journal | View Issue

Cite this: *Environ. Sci.: Atmos.*, 2023, **3**, 1778

NO_3 reactivity measurements in an indoor environment: a pilot study†

Patrick Dewald, Jos Lelieveld and John N. Crowley *

We present the first direct indoor measurements of VOC-induced nitrate radical (NO_3) reactivity (k^{NO_3}) together with measurements of nitric oxide (NO), nitrogen dioxide (NO_2), ozone (O_3) and dinitrogen pentoxide (N_2O_5) inside a laboratory during a four-day period in October 2021 in a suburban area (Mainz, Germany). Indoor mixing ratios of O_3 ranged from <2–28 ppbv and those of NO_2 from 4.5–27 ppbv. The rapid ventilation of the room (air change rates of ~4 h^{-1}) meant that indoor mixing ratios mirrored the variability in NO_2 and O_3 outdoors. NO_3 production rates were between <0.02 and 0.12 pptv s^{-1} with indoor N_2O_5 mixing ratios increasing to 4–29 pptv during five NO-depleted day- or nighttime periods when k^{NO_3} was between 0.04 and 0.2 s^{-1}. Steady-state calculations resulted in a peak NO_3 mixing ratio of 6 pptv. A comparison of measured N_2O_5 mixing ratios to those derived from steady-state calculations and the equilibrium coefficient for the NO_2, NO_3, N_2O_5 system showed very good agreement, indicating that heterogeneous reactions do not contribute significantly to the overall NO_3 loss rate (L_{NO_3}). During these five periods, NO_3 was mostly lost to NO and VOCs, the latter contributing on average 65% to L_{NO_3}. This pilot study underlines the necessity of further indoor NO_3 reactivity measurements and that the nitrate radical can be a significant indoor oxidizing agent when the room is sufficiently ventilated during episodes of moderate outdoor air pollution.

Received 13th September 2023
Accepted 3rd November 2023

DOI: 10.1039/d3ea00137g

rsc.li/esatmospheres

Environmental significance

The nitrate radical (NO_3), formed by the reaction between ozone (O_3) and nitrogen oxide (NO_2), is an important nocturnal oxidant of unsaturated volatile organic compounds in the atmosphere. While its effect on the atmospheric lifetime of NOx has been extensively studied outdoors, indoor studies of NO_3 are very limited. The short atmospheric lifetime of NO_3 makes its detection challenging. We demonstrate the first direct measurement of NO_3 reactivity indoors, providing an alternative way to assess NO_3 concentrations under polluted conditions. Our measurements suggest that NO_3 can be the dominant indoor oxidant of limonene, which is often released indoors owing to its presence in cleaning agents. This study emphasizes that NO_3 chemistry can significantly impact indoor air quality.

1 Introduction

Since a great fraction of human lifetime is spent indoors, the composition of indoor air can have a significant impact on human health.[1] Analogous to outdoor environments, the major indoor oxidants are ozone (O_3), the hydroxyl radical (OH) and the nitrate radical (NO_3).[2–5] NO_3 is produced by the oxidation of nitrogen dioxide (NO_2) by ozone (O_3), both of which are usually present in indoor air from ventilation of outside air:[4]

$$NO_2 + O_3 \rightarrow NO_3 + O_2 \quad (R1)$$

Dinitrogen pentoxide (N_2O_5) is formed *via* reaction of NO_3 and NO_2 and is in thermal equilibrium with both:[6]

$$NO_3 + NO_2 + M \rightarrow N_2O_5 + M \quad (R2)$$

$$N_2O_5 + M \rightarrow NO_3 + NO_2 + M \quad (R3)$$

In outdoor environments during the day, NO_3 is removed rapidly by reaction with NO (R4) and *via* photolysis by sunlight ((R5a) and (R5b)).[7]

$$NO_3 + NO \rightarrow 2\ NO_2 \quad (R4)$$

$$NO_3 + h\nu\ (\lambda \approx 400 - 640\ nm) \rightarrow NO_2 + O \quad (R5a)$$

$$NO_3 + h\nu\ (\lambda \approx 585 - 640\ nm) \rightarrow NO + O_2 \quad (R5b)$$

NO_3 photolysis rates indoors are sufficiently diminished compared to outside so that (R5a) and (R5b) can be neglected and NO_3 gains in importance, relative to O_3 and OH, as an oxidizing agent.[4,10,11] As evident from (R1), NO_3 production (and its subsequent chemistry) relies on the presence of O_3 and NO_2. Elevated indoor ozone (and NO_x) levels are particularly common in urban buildings equipped with ventilation systems or when

Department of Atmospheric Chemistry, Max-Planck-Institute for Chemistry, 55128 Mainz, Germany. E-mail: john.crowley@mpic.de

† Electronic supplementary information (ESI) available. See DOI: https://doi.org/10.1039/d3ea00137g

windows are open,[12,13] so that indoor NO_3 production rates become significant. Indoor ozone can be consumed by NO (R6) in poorly ventilated, residential environments,[14] where a major (indoor) source of NO is gas cooking.[4]

$$NO + O_3 \rightarrow NO_2 + O_2 \quad (R6)$$

Unsaturated volatile organic compounds (VOCs) such as terpenes, which are highly reactive towards NO_3,[15] are often abundant in indoor environments as they are present in detergents and cleaning agents.[16] In some environments (*e.g.* forested regions), reactions with unsaturated hydrocarbons not only become the dominant NO_3 removal process at night, but even compete with (R4), (R5a) and (R5b) during the day.[8,9] In addition, the reaction of NO_3 with VOCs (R7) leads (among other products) to the formation of alkyl nitrates ($RONO_2$) or nitric acid (HNO_3), which, in outdoor environments can transfer to the particle phase leading to secondary organic aerosols (SOA) and/or particulate nitrate.[17,18]

$$NO_3 + VOCs\ (+O_2) \rightarrow\rightarrow \text{products } (e.g.\ RONO_2,\ HNO_3) \quad (R7)$$

While the impact of O_3 and OH on indoor air quality has been extensively investigated,[3,14,19,20] the number of studies examining the role of the nitrate radical in indoor environments is very limited. Along with some model calculations and steady-state calculations which suggest that indoor NO_3 levels are below 0.04 parts per trillion by volume (pptv),[13,21–24] only a few direct measurements of NO_3 or its equilibrium partner N_2O_5 are available.[25–27] Arata *et al.*[26] detected several pptv of NO_3 in a poorly-ventilated residential kitchen when the NO_3 production rate was artificially enhanced by continuous addition of "synthetic" O_3 (up to 40 parts per billion by volume, ppbv). Detectable mixing ratios of N_2O_5 and NO_3 in the lower pptv range have been reported for ventilated rooms (exchange rates of 3.8 h^{-1} and 7 h^{-1}) in an office building and an athletic facility.[25,27]

This limited number of studies indicates that, in poorly ventilated rooms, high NO_3 loss rates make it difficult to assess the impact of the nitrate radical yet no direct indoor NO_3 reactivity measurements have been reported. In addition, with the outbreak of the COVID-19 pandemic, rapid ventilation of indoor environments has become increasingly important to reduce viral loads.[28,29] Rapid ventilation of outside air results in the transport of photochemically generated O_3 and NO_x into the indoor environment. Clearly, indoor measurement of NO_3 mixing ratios, NO_3 production rates and NO_3 reactivity would thus help to assess the fate of NO_3 radicals in such an environment. In this study, we report the first measurements of VOC-induced NO_3-reactivity along with mixing ratios of the nitrogen oxides NO, NO_2, NO_3 and N_2O_5 together with O_3 from a well-ventilated laboratory over a weekend period in October 2021 in Mainz (Germany). Quantifying VOC-induced NO_3 reactivity together with the above-mentioned set of measurements enables identification of the dominant NO_3 loss processes which may allow qualitative conclusions about the formation of organic nitrates indoors to be drawn. The purpose of this study is thus to evaluate whether NO_3 reactivity measurements provide us with new insights into indoor oxidation processes.

2 Experimental

The laboratory used in this study has a volume of ~220 m^3 (floor area = 61 m^2) and was mostly unoccupied during the measurement period in order to reduce the impact of the human emissions on the observations. The room itself is located at the Max-Planck-Institute for Chemistry (MPIC) that is situated in direct vicinity to commercial, residential and university buildings. Busy two- and four-lane roads leading to the city center of Mainz (5 km, 217 000 inhabitants) are adjacent to the institute. Mainz is part of the densely populated and industrialized Rhine-Main area close to Frankfurt and Wiesbaden. A ventilation system, that was continuously operated in "night-mode" (*i.e.* reduced air change rate, see Supplement S1†) during the study period constantly replenished the room with urban (polluted) air from outside. The air change rate (k_{change}) was estimated using a tracer-gas approach[30] in which limonene or 2,3-dimethyl-2-butene was released into the laboratory and its decay in concentration was monitored. The concentration of limonene or 2,3-dimethyl-2-butene was not measured directly but by the change (reduction) in NO_3 reactivity as their mixing ratios decreased mainly due to exchange with outdoor air. Following a phase of mixing (<1 min) initial concentrations of ≈ 200 pptv (for limonene) decrease to roughly zero in ≈ 30 min. The decay of limonene and of 2,3-dimethyl-2-butene is exponential, enabling decay constants (or air change rate constants) of 5.76 h^{-1} (limonene) and 4.3 h^{-1} (2,3-dimethyl-2-butene) to be derived. The faster decay term for limonene is likely related to its indoor oxidation and wall loss, which are both expected to be more rapid than for 2,3-dimethyl-2-butene. Due to the bias caused by deposition and chemical loss processes, the values derived by our approach serve as an upper limit of the true air change rate. In the case of limonene, gas-phase losses contribute ≈ 30% to the overall decay rate. The air change rate of our laboratory during the measurement period was less than 4 h^{-1}. The procedure and results of the air change rate determination are found in more detail in the Supplement (S1†). Note that a more volatile and less reactive tracer such as carbon dioxide (CO_2), which is readily available through respiration and can be detected by inexpensive sensors, represents an alternative tracer.

The east side of the room featured windows to an inner courtyard. Light entering the room through the permanently closed windows was attenuated by a fine-meshed sunscreen. The room lights (fluorescent strip-lamps) were turned off during the entire period. Spectral-radiometric measurements verified that NO_3 photolysis rates (J_{NO_3}) resulting from the attenuated daylight (<10^{-6} s^{-1}) were insignificant (see Supplement, Fig. S2†).

The laboratory was equipped with four instruments described below, each one connected to a central exhaust system. The NO bottles used to run the cavity ring-down spectrometers (CRDS) were stored in a separate, ventilated safety cabinet. All gas lines were thoroughly checked for leakages. By

avoiding potential laboratory (chemical) emissions, the composition of the air should thus be comparable to other ventilated rooms. The measurements were carried out at the institute during a four-day period from Friday to Tuesday in October 2021 during which the maximum outdoor daytime and nighttime temperatures were 14 °C and 5 °C, respectively. The weather during the weekend was dominated by clouds and fog, the only extended sunny period was on October 16 between 07:00 and 15:00 UTC.

2.1 NO_3 reactivity

The NO_3 reactivity (k^{NO_3}) was directly measured with a cavity ring-down spectrometer that was coupled to a flowtube (FT-CRDS) as detailed in Liebmann *et al.*[31] After accounting for the impact of NO_x (see below), this instrument quantifies the total gas-phase NO_3 reactivity (*i.e.* the inverse of the NO_3 lifetime) towards VOCs, so that k^{NO_3} is equal to the summed first-order loss rate $\Sigma k_i[VOC]_i$ with the concentration of a VOC $[VOC]_i$ and the corresponding rate coefficient k_i for its reaction with NO_3 (R7). A commercial zero-air generator (CAP 180, Fuhr GmbH) provides 400 standard (STP) cubic centimeters per minute (sccm) of zero-air which is passed over a mercury lamp (Penray) to generate O_3 at *ca.* 400 ppbv. This flow is mixed with a flow of NO (3 sccm of 1 parts per million by volume (ppmv) in N_2, Air Liquide) and directed through a thermostated Teflon-coated (FEPD 121, Chemours) reactor (30 °C, 1.3 bar). During the residence time of *ca.* 5 min, O_3 sequentially oxidizes NO to NO_2 (R5) and then to NO_3 (R1), which reacts with NO_2 to form N_2O_5 (R2). Passing the gas through a 15 cm long piece of PFA (perfluoroalkoxy) tubing (outer diameter (OD) of 1/4 in. = 0.635 cm) heated to 140 °C converts N_2O_5 to NO_3 and NO_2 (R3). The flow containing NO_3 is then mixed with 2800 sccm synthetic or ambient air and directed through a Teflon-coated (FEPD 121, Chemours) flowtube, where the gas-mixture has a time of 11 s to react. The NO_3 that survives the flowtube is quantified using cavity ring-down spectroscopy (CRDS) at a wavelength of 662 nm. The basic principle of the instrument thus relies on comparing the level of synthetic NO_3 in zero-air (*i.e.* total NO_3 reactivity = 0 s^{-1}), to those in indoor air. The ring-down time in the absence of NO_3 was determined by the periodic addition of sufficient NO (3 sccm of 100 ppmv NO in N_2, Air Liquide) to titrate the NO_3 completely. Zero-air was humidified to match indoor-air humidity using a permeation-tube based humidification system (PermaPure, MH-070-24F-4) filled with deionized water (LiChrosolv, Merck). Indoor air was sampled through 1 m 1/4 in. (OD) PFA tubing equipped with a Teflon membrane filter (Pall Corp., 47 mm, 0.2 μm pore) to protect the mirrors and through a 2 L (uncoated) borosilicate glass flask heated to 45 °C to remove both ambient NO_3 and N_2O_5, which would bias the measurement.

Indoor air was dynamically diluted with zero-air during periods with highly reactive ambient air, which extends the upper limit of measurable reactivities to 1.7 s^{-1}. The variability of the NO_3 source and cavity instabilities results in a lower limit of detection (LOD) of 0.006 s^{-1} and contribute ~18% to the measurement uncertainty.

As described by Liebmann *et al.*,[31] the presence of NO, NO_2, O_3 (and thus reactions ((R1–R4) and (R6) and (R7)) and NO_3 losses on the walls of the flowtube (NO_3 wall loss rate = 0.001 s^{-1}) require numerical simulations in order to extract the NO_3 reactivity (k^{NO_3}) that can be attributed to VOCs (R7). Due to the numerical correction procedure, the total uncertainty of the measurement is dependent on the ratio of ambient NO_2 and k^{NO_3}.[31] Note that conversion of NO to additional NO_2 *via* (R6) in the flowtube affects NO_2/k^{NO_3} which is why accounting for the impact of NO becomes significant in polluted conditions not only because of (R4). If, for example, a reactivity of 0.15 s^{-1} is measured in the presence of 12 ppbv NO_2, the additional uncertainty introduced by the numerical simulations would be ~24%, leading to a total measurement uncertainty (TMU) of 30% which corresponds to the median TMU of this instrument during the study.

2.2 NO_3 and N_2O_5

Ambient NO_3 and N_2O_5 mixing ratios were monitored using the two 662 nm cavities of the five-channel cavity ring-down spectrometer (5Ch-CRDS), described by Sobanski *et al.*[32] In this instrument, N_2O_5 is quantitatively dissociated to NO_3 (R3) by passing the sample air through a Teflon-coated glass tube heated to 95 °C prior to entering the cavity at the same temperature. The heated cavity consequently detects the sum of $NO_3 + N_2O_5$. Similar to the FT-CRDS, the "baseline" (*i.e.* the ring-down time in the absence of the absorbing species) was determined by adding NO to the cavity (6 sccm of 100 ppmv NO in N_2, Air Liquide). Air was sampled at 15 standard (STP) liters per minute (SLPM) through 10 cm of 1/4 in. (OD) PFA tubing and a Teflon membrane filter (Pall Corp., 47 mm, 0.2 μm pore) with the heated cavity sampling 7 SLPM and the unheated one 8 SLPM. To reduce NO_3 loss through the inlet, an automatic filter changer normally replaces the inlet filter every hour. Unfortunately, the filter changer was not available during the measurement period. The data was corrected for cavity losses of NO_3, the effective NO_3 cross-section at both cavity temperatures and the impact of the mirror purge gas flow as described in Sobanski *et al.*[32] Taking the standard deviation (2σ) from the baseline variability of the whole 10 min-averaged data set results in LODs of 0.9 pptv and 1.5 pptv for NO_3 and N_2O_5, respectively. The total uncertainty associated to the NO_3 and N_2O_5 measurements is 25% and 28%, respectively.

2.3 NO and NO_2

NO and NO_2 were measured with a two-channel, cavity ring-down spectrometer[33] operated at 405 nm. One cavity directly samples ambient air to detect NO_2, while the other samples *via* additional tubing (1 m 1/2 inch (OD) PFA) that forms a reaction volume in which NO is oxidized to NO_2 *via* the addition of ~3 ppmv O_3 (R6). The second cavity thus detects the sum of NO and NO_2 so that NO mixing ratios were derived by the difference signal. Each cavity sampled indoor air at a flow of 2 SLPM through ~2 m 1/2 in. (OD) PFA tubing and a Teflon membrane filter (Pall Corp., 47 mm, 0.2 μm pore). Based on the noise level and the variability in the baseline, the LODs of the NO and NO_2

measurements are 132 pptv and 57 pptv with associated uncertainties of 11% and 9%, respectively.

Since the correction of the NO_3 reactivity measurements requires accurate NO_2 measurements, NO_2 mixing ratios were additionally monitored with a cavity of the 5Ch-CRDS operated at 405 nm. A comparison of both NO_2 measurements is presented in the Supplement (Fig. S3†) and reveals excellent agreement between the two-channel and five-channel instruments. As both instruments were placed in opposed corners of the laboratory, this comparison also confirms that the air in the room is well mixed.

2.4 O_3 and other auxiliary measurements

Ozone mixing ratios were measured with a commercial ozone monitor (2B Technologies, model 205) based on UV absorption. The instruments detects O_3 mixing ratios > 2 ppbv with an uncertainty of 5%.

Relative humidity (RH) and temperature (T) measurements were monitored with the NO_3 reactivity setup (see 2.1) by separately sampling 500 sccm ambient air over a commercial hygrometer (Innovative Sensor Technology, HYT939) with an accuracy of ±1.8% (RH) and ±0.2 °C (T). Total (*i.e.* non-size-segregated) particle number densities were sporadically measured after the pilot study using a condensation particle counter (CPC, TSI, model 3025a).

Indoor photolysis frequencies were determined using a spectral-radiometer (Metcon GmbH) with a single monochromator and 512 pixel CCD array as a detector (275–640 nm). The thermostated monochromator-detector unit was attached *via* a 10 m optical fiber to an integrating hemispheric quartz dome that was placed at a height of *ca.* 2 m in the center of the room. Light fluxes were converted to photolysis rate constants for NO_3 ((R5a) and (R5b), J_{NO_3}) and NO_2 (J_{NO_2}) using molecular parameters recommended by the IUPAC and NASA evaluation panels.[34,35]

3 Results and discussion

A time-series of the mixing ratios of NO, NO_2, O_3, NO_3 and N_2O_5 as well as RH, T and k^{NO_3} is given in Fig. 1 together with calculated quantities (*e.g.* production and loss rates of NO_3) that are discussed in section 3.2. Within the measurement period, the relative humidity varied between 24% and 36% at a fairly constant temperature of 297–298 K (panel a). NO (<132 pptv to 41 ppbv, panel b), NO_2 (4.5 to 27 ppbv, panel b) and O_3 (<2 ppbv to 28 ppbv, panel c) mixing ratios were quite variable. During

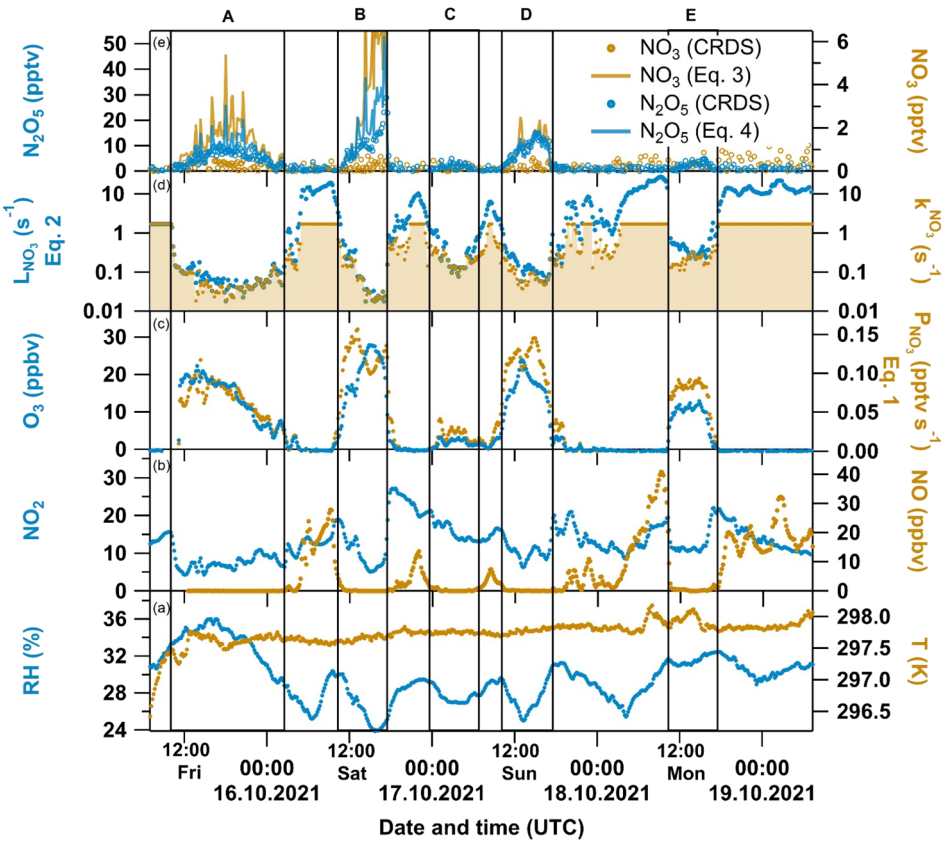

Fig. 1 Overview of directly measured and derived quantities during a weekend period inside a ventilated laboratory: (a) relative humidity RH (blue, left axis) and temperature T (orange, right axis); (b) NO_2 (blue, left axis) and NO (orange, right axis) (c) O_3 (blue, left axis) and NO_3 production rate P_{NO_3} from (Eq. 1) (blue, right axis); (d) Total NO_3 loss rate L_{NO_3} from (Eq. 2) (blue, left axis) and NO_3 reactivity k^{NO_3} (LOD of 1.7 s^{-1}, orange with same-coloured shaded area to mark its contribution to L_{NO_3}); (e) N_2O_5 (blue circles, left axis), calculated N_2O_5 from (Eq. 4) (blue line, left axis), NO_3 (orange circles, right axis) and calculated NO_3 from (Eq. 3) (orange line, right axis).

the periods in which NO was high, likely a result of nearby automobile emissions, the NO_3 reactivity exceeded the instrument's upper LOD of 1.7 s^{-1} (panel d), which was reached when the NO mixing ratio exceeded 2.5 ppbv.

We have divided the measurements into five periods (A–E in Fig. 1), during which N_2O_5 mixing ratios (panel e) were >2 pptv and NO mixing ratios were close to or below the LOD, whereas O_3 mixing ratios were large. The anti-correlation between NO and O_3 is readily understood considering the efficient conversion of NO to NO_2 *via* (R6), which has the following consequences: (1) The presence of O_3 (together with NO_2) enables the production of both NO_3 and N_2O_5. (2) The lack of NO leads to lower NO_3 reactivities (*i.e.* higher NO_3 lifetimes) of between 0.04 to 0.2 s^{-1}. This is reflected in measurable amounts of N_2O_5 (up to 29 pptv) during period B.

In this study, NO_3 remained undetected. Considering the thermal equilibrium between NO_2, NO_3 and N_2O_5 ((R2) and (R3)) and the measured NO_2 and N_2O_5 mixing ratios, this is contradictory to calculations using evaluated rate coefficients for k_2 and k_3,[35] which indicated the presence of 2–4 pptv NO_3. The most likely explanation is that NO_3 (a reactive radical) was lost during sampling through the inlet tubing and filter, while both N_2O_5 and NO_2 pass almost loss-free through the system. After use over the 4 days period, the inlet filter was clearly contaminated with dark-coloured particles, presumably black-carbon. A picture of this filter in comparison to an unused filter is shown in the Supplement (Fig. S4†). A previous study[36] on the interaction of NO_3 and N_2O_5 with urban aerosols collected on filter samples at the same location showed no measurable uptake for N_2O_5, whereas NO_3 was lost efficiently with $\gamma(NO_3)/\gamma(N_2O_5) > 15$, where γ is the net-uptake coefficient for heterogeneous loss.

Outdoors, NO_3 and N_2O_5 are usually only observed during nighttime due to NO_3 photolysis rates of typically up to 0.17 s^{-1} at noon,[7] whereas in this study N_2O_5 was detected independently of the diel cycle. In Fig. 1, period A covers a daytime–nighttime transition, the N_2O_5 peaks in periods B, D and E are around noontime, while period C is a nighttime period. However, an air change rate of 4 h^{-1} is sufficient to entrain N_2O_5 originating from outside into the laboratory especially at night. To assess the potential impact of outdoor N_2O_5 on our measurement, we compare the calculated *in situ* indoor N_2O_5 production rate $P_{indoor}(N_2O_5)$ with the production rate $P_{outdoor}(N_2O_5)$ caused by infiltration of N_2O_5 originating from outside. According to (R2) and (Eq. 4), $P_{indoor}(N_2O_5)$ is equal to $k_2[NO_2][NO_3] \approx k_1k_2[NO_2]^2[O_3]/L_{NO_3}$. Calculation of $P_{indoor}(N_2O_5)$ from our measurements of NO_2, O_3, NO and k^{NO_3} results in values of 0.1–2.1 pptv s^{-1} during periods A–E. Schuster *et al.*[37] reported nighttime N_2O_5 mixing ratios outside the institute in October 2007 of up to 80 pptv which would result in an production rate $P_{outdoor}(N_2O_5) = [N_2O_5]_{outdoor} \times k_{change}$ of $\approx$ 0.01 pptv s^{-1}. Unless several hundreds of pptv of N_2O_5 were constantly abundant outside, $P_{outdoor}(N_2O_5)$ is very unlikely to affect our N_2O_5 levels measured inside.

3.1 Comparison of indoor and outside air

With an air change rate of up to 4 h^{-1}, the composition of the air in the laboratory is strongly influenced by that outside. Fig. 2 compares the indoor mixing ratios of O_3 and NO_2 to those from a local air-quality measurement station[38] located in Mainz-Mombach, *ca.* 4 km north of the Max-Planck-Institute. For both trace gases, the indoor/outdoor diel profiles are very similar. Outdoor O_3 is close to zero at nighttime, which is the result of deposition to surfaces and also reaction with NO forming NO_2 (R6). Outdoors, NO_2 is rapidly photolysed during the day (R8) to re-generate O_3 (R9), whereas indoor photolysis rates for NO_2 (J_{NO_2}) are very low (see Fig. S2 in the Supplement†) and there are no significant *in situ* sources of O_3 in the laboratory. The availability of O_3 indoors thus depends entirely on exchange with outdoor air and the strong co-variance is expected. Outdoors, the nighttime increase in NO_2 (resulting from the oxidation of locally emitted NO) results in rapid formation of O_3 at the start of the day as NO_2 is photolysed (to $O(^3P)$ and thus O_3).

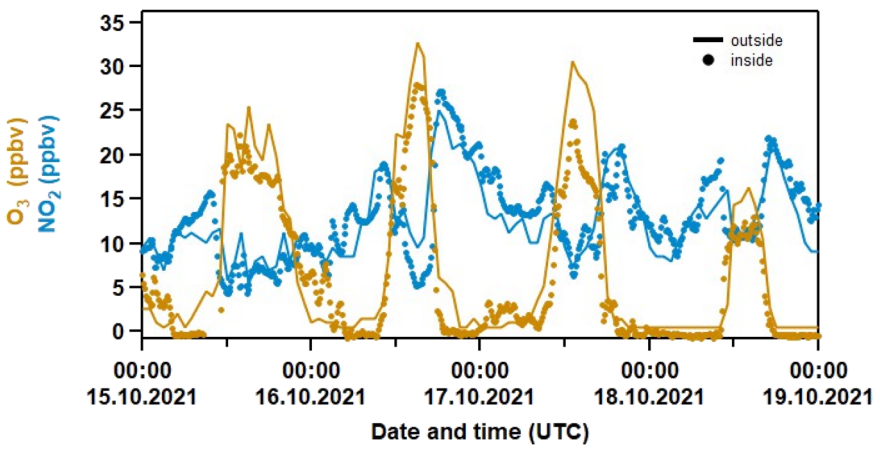

Fig. 2 Measurements of O_3 and NO_2 inside the laboratory (dots, 10 min data) and outside at a station in Mainz–Mombach (solid line, 1 h data). The outdoor data was taken from the German Environment Agency[38] and converted from μg cm^{-3} to ppbv using a pressure of 760 Torr and a temperature of 298 K.

$$NO_2 + h\nu \rightarrow NO + O(^3P) \quad \text{(R8)}$$

$$O(^3P) + O_2 + M \rightarrow O_3 + M \quad \text{(R9)}$$

There is no obvious lag in the indoor O_3 data at sunrise compared to outdoors, which implies that the air change rate is more rapid than the production and loss terms for O_3. The indoor-to-outdoor ratio (I/O) of O_3 and NO_2 was obtained by measuring both NO_2 and O_3 sequentially inside the laboratory and directly outside by passing the inlet through a port in the wall (Fig. 3). In this case, I/O(O_3) was determined to be 0.63 ± 0.03 (1σ). Note that windows are shut at all times in the laboratory, and that outdoor air passes through a compressor, metal piping and filters before entering the labs so O_3 is expected to be lost, which explains the lower than unity indoor/outdoor ratio. An average I/O of 0.25 was recently reported in a review summarizing measurements in *ca.* 2000 indoor environments.[14]

I/O(O_3) can be assessed by assuming that the air change rate k_{change} and surface removal rate $k_{surface}$ of O_3 are much faster than its outdoor variability so that I/O(O_3) = $k_{change}/(k_{change} + k_{surface})$.[12] Using an air change rate of 4 h^{-1} and a surface removal rate for O_3 as reported for a laboratory environment of 2.5 h^{-1},[12] I/O(O_3) = 0.62 is derived, which is close to the observed value. However, I/O(O_3) is affected by several parameters such as the air change rate, abundance of NO, loss rate on indoor surfaces (highly dependent on the material), transmission loss through ventilation systems and the presence of humans.[14] The values of $k_{surface}$ may consequently be very different for two non-identical laboratories. Since indoor O_3 only reached elevated levels when NO ≤ 150 pptv resulting in a maximum O_3 loss rate of 0.25 h^{-1}, the contribution of (R6) was neglected.

As mentioned above, the oxidation of NO by O_3 not only leads to O_3 loss, but also to formation of NO_2. As shown in Fig. 3, the indoor mixing ratios of NO_2 (1800–2100 pptv) were indeed higher than outside (1100 to 1700 pptv). The high variability in NO_2 outside makes it impossible to accurately quantify a value for I/O(NO_2), which is highly dependent on the availability of indoor NO_2 sources, the ratio between k_{change} + $k_{surface}$ (similarly to O_3), season (photochemistry) and location. Models and long-term experiments show that I/O(NO_2) is often above or close to unity in non-domestic, strongly ventilated rooms in urban areas similar to our laboratory.[39,40]

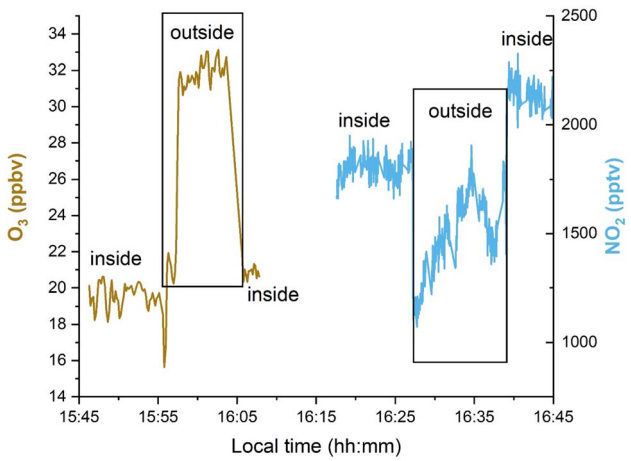

Fig. 3 Sequential measurements of O_3 and NO_2 inside and outside the laboratory on the 21st October 2021.

In summary, Fig. 2 and 3 underline (1) that (for a given ventilation rate) the indoor abundance of the NO_3 precursors (NO_2 and O_3) are mainly determined by the air composition outside and (2) that (R6), similarly to outdoors, explains the distinct anti-correlation between O_3 and NO_x measured indoors as observed in Fig. 1.

In this laboratory environment, in which the indoor air is supplied by a compressor/filter system, the particle concentration is greatly reduced compared to outdoors. A few checks (after our pilot study) showed that the typical number density indoor-to-outdoor ratio, I/O(N_{part}), was close to 0.1. As shown below, the low particle number density results in low aerosol surface areas, hence leading to insignificant losses of *e.g.* N_2O_5 or NO_3 to particles in ambient air compared to other surfaces and/or reactants. Nevertheless, accumulation of ambient particles on our inlet filter with time results in quantitative NO_3 removal prior to entering our cavity.[36] The PTFE membrane filters are usually changed (automatically) on an hourly basis during measurements to avoid this issue.[32,41]

3.2 Measured *versus* calculated NO_3 and N_2O_5 mixing ratios

NO_3 and N_2O_5 mixing ratios can be calculated from a stationary-state approximation if measurements of NO_2 and O_3 mixing ratios as well as NO_3 reactivity are available:[41–47] By using the rate coefficient k_1 for the reaction between NO_2 and O_3 (R1) and the mixing ratios of O_3 and NO_2, the NO_3 production rate (P_{NO_3}) can be assessed:

$$P_{NO_3} = k_1[NO_2][O_3] \quad \text{(Eq. 1)}$$

In our analysis, the NO_3 reactivity k^{NO_3} is corrected for the impact of NO_x. Thus, in order to derive the overall NO_3 loss rate L_{NO_3} (assuming only the overall gas-phase loss rate k_{gas} is relevant compared to heterogeneous loss rate k_{het}), the pseudo-first-order loss rate constant for reaction with NO has to be added:

$$L_{NO_3} = k_{gas} + k_{het} \approx k^{NO_3} + k_4[NO], \quad \text{(Eq. 2)}$$

With k_4 being the rate coefficient for the reaction between NO and NO_3 (R4). In stationary state, *i.e.* $d[NO_3]/dt \approx 0$ the NO_3 loss rate is in balance with its production rate (Eq. 3) and its steady-state concentration $[NO_3]_{ss}$ can be calculated:

$$[NO_3]_{ss} = \frac{P_{NO_3}}{L_{NO_3}} = \frac{k_1[NO_2][O_3]}{k^{NO_3} + k_4[NO]} \quad \text{(Eq. 3)}$$

This approximation is valid as long as the system is in equilibrium ((R2) and (R3)), NO_3 loss rates are sufficiently large and NO_2 does not vary too much on short time-scales.[48,49] The thermal equilibrium constant $K_{eq} = k_2/k_3$ (ref. 35) enables derivation of N_2O_5 mixing ratios:

$$[N_2O_5]_{eq} = K_{eq}[NO_2][NO_3]_{ss} \quad \text{(Eq. 4)}$$

The NO_3 production and loss rates, and steady-state mixing ratios of NO_3 and N_2O_5 calculated using (Eq. 1) to (Eq. 4) are displayed in Fig. 1. When both O_3 and NO_2 were present (*i.e.* when O_3 was not removed by NO) the NO_3 production rates were between 0.02 and 0.12 pptv s^{-1}. Since the abundance of O_3 was the limiting factor in NO_3 production in this study, P_{NO_3} mostly follows the diel pattern of O_3 (Fig. 1, panel c). During NO-rich periods, O_3 is not only entirely depleted (so that $P_{NO_3} \approx 0$ pptv s^{-1}), but L_{NO_3} also increases to 10 s^{-1} (panel d), which is why neither NO_3 nor N_2O_5 was expected. Furthermore, Fig. 1 (panel e) shows good agreement between measured and calculated N_2O_5 mixing ratios. At higher N_2O_5 mixing ratios, up to 6 pptv of NO_3 would have been present at equilibrium (with NO_2 and N_2O_5), which would have been detectable by our instrument. The lack of a NO_3 signal is attributed to its loss on a contaminated filter (see above).

In order to analyze the conditions under which indoor N_2O_5 is observable, we focus on period D (Fig. 4) which we consider representative of all periods in which N_2O_5 was detected. The uncertainties in P_{NO_3}, L_{NO_3}, $[NO_3]_{ss}$ and $[N_2O_5]_{eq}$ were derived from propagation of the uncertainties associated with the measurements (see section 2) as well as with the rate coefficients k_1 (15%) and K_{eq} (20%).[34,35] In Fig. 4, N_2O_5 (panel e) starts to increase around 10:00 UTC and O_3 mixing ratios (panel c) increase from < 2 ppbv to 20 ppbv (at 14:00). At the same time, NO (panel b) decreases from 3 ppbv to close to, or below the LOD so that NO_3 loss rates (panel d) are around 0.04–0.1 s^{-1}. The NO_3 production rate (panel c) of *ca.* 0.06 pptv s^{-1} (circa 20 ppb O_3 and 10 ppbv NO_2) is sufficient to generate detectable amounts of NO_3/N_2O_5 (panel e). These observations emphasize that the presence of N_2O_5 (and NO_3) goes hand-in-hand with O_3 mixing ratios that are sufficient for removal of NO (and its subsequent conversion to NO_2). As indicated in section 3.1, the abundance of indoor NO_2 and O_3 is mostly determined by their outdoor mixing ratios and the air change rate. Between 14:00 and 16:00 UTC in Fig. 4, we have 2 pptv NO_3 and 20 ppbv O_3. If we assume an OH concentration of 7×10^5 molecules cm^{-3},[20,50] the loss rate constants for an indoor VOC such as limonene would be 5.91×10^{-4} s^{-1} (NO_3 loss), 1.08×10^{-4} s^{-1} (O_3 loss) and 1.15×10^{-4} s^{-1} (OH loss). During period D, NO_3 is thus the major oxidant of limonene and presumably other unsaturated compounds that display similar reactivity to NO_3. In contrast to the reaction with O_3 and OH which form carbonyl compounds (*e.g.* limona ketone, 4-acetyl-1-methyl-1-cyclohexene) and peroxy acetyl nitrate ($CH_3C(O)O_2NO_2$, PAN) indoors,[51] the NO_3-initiated oxidation of limonene results in the formation of alkyl nitrates ($RONO_2$) in high yields (30–67%).[35] Note that the reaction with NO_3 would only contribute *ca.* 30% to the total VOC loss rate when the maximum air change rate of 4 h^{-1} is taken into account.

The good agreement between the measured and calculated N_2O_5 mixing ratios (Fig. 4) is further examined in Fig. 5 in which these quantities are plotted against each other. For this, mixing ratios at or below the LOD have been removed. A bivariate,

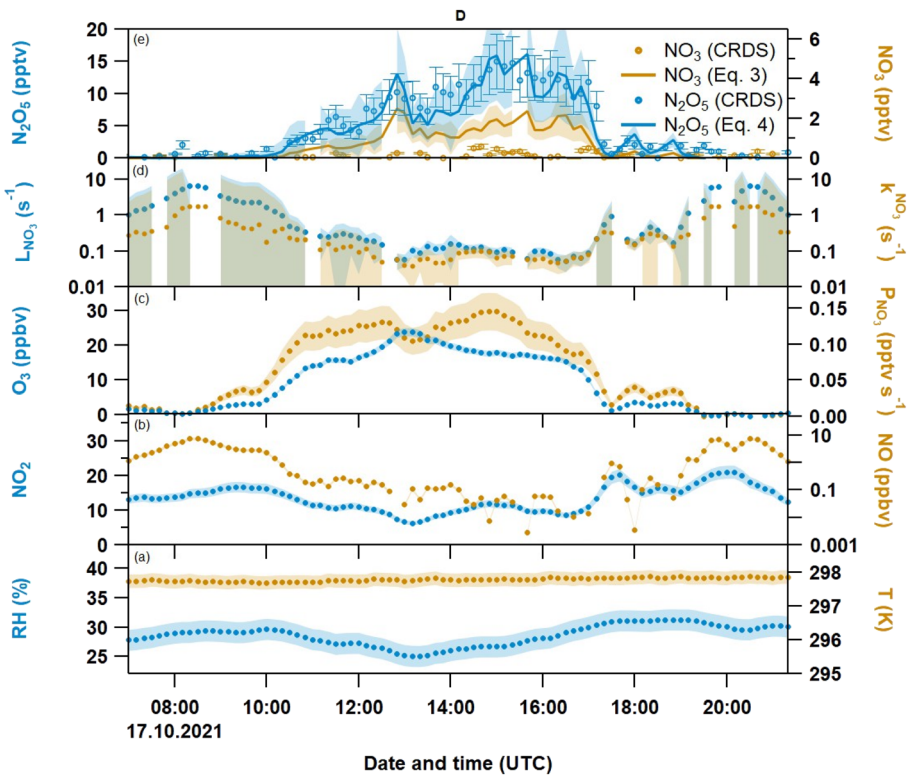

Fig. 4 Same as Fig. 1, but expanded to display period D. Total uncertainties are shown by shaded areas in the same color as the corresponding traces. In the case of directly measured NO_3 and N_2O_5, the uncertainties are shown as error bars.

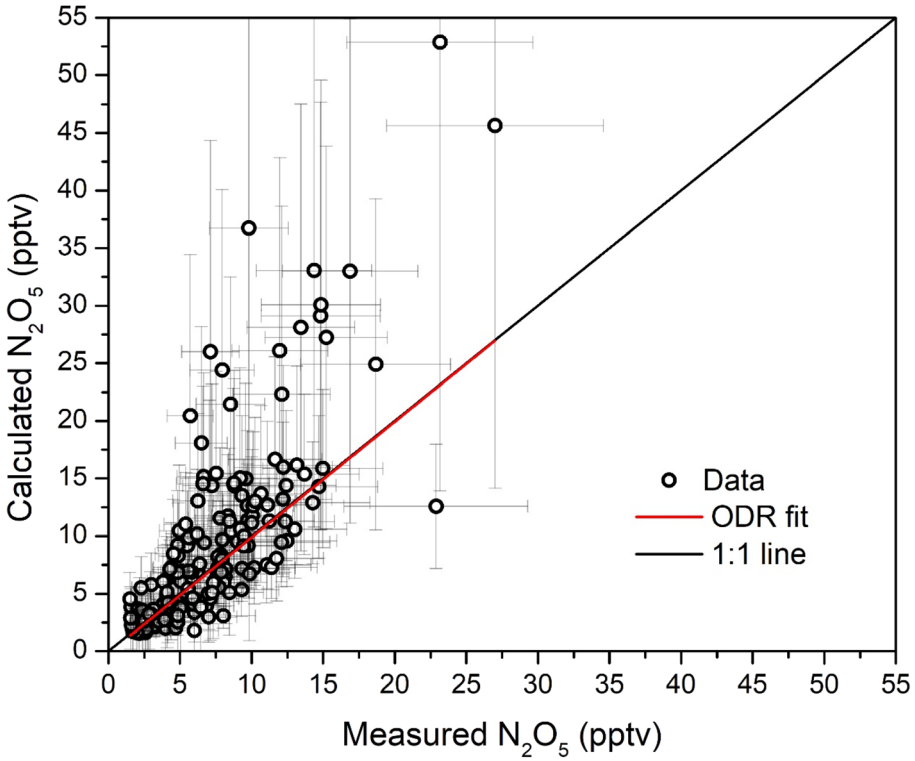

Fig. 5 N_2O_5 mixing ratios calculated from (Eq. 4) *versus* those directly measured. The red solid line shows an orthogonal distance regression (ODR,[57] slope: 1.00 ± 0.09, intercept: (−0.16 ± 0.34) pptv, Pearson correlation coefficient r = 0.8) while the black line denotes ideal 1 : 1 agreement.

linear regression yields an intercept of (−0.16 ± 0.34) pptv and a slope of 1.00 ± 0.09, indicating very good agreement within associated uncertainties. As heterogeneous loss processes of both N_2O_5 and NO_3 are neglected in the calculation of N_2O_5 mixing ratios, and reactions of NO_3 with RO_2 (or other radicals) do not contribute to the measured loss term, we conclude that (within the associated uncertainty of this analysis), the loss of NO_3 (and thus indirectly N_2O_5) is dominated by reactions with VOCs and NO. The uptake of N_2O_5 to aqueous particles can be an important term outdoors, but in an indoor environments which is supplied with fresh-air *via* filters, particle concentrations indoors are too low for this to contribute significantly (see section 3.1). In addition, the RH was relatively low so that the water content of aerosol particles is expected to be minor, which lowers the N_2O_5 uptake coefficient.[52]

During period B (see Fig. 1, upper panel) a greater deviation between measured and calculated N_2O_5 mixing ratios is observed, which results in some of the scatter in Fig. 5. Period B is the only sunny period of the measurement period and an increase of 0.016 s^{-1} in the NO_3 loss rate constant would be necessary to bring measured and calculated values into agreement. Such a reactivity would be caused by just 25 pptv of NO, which is below the LOD of the NO instrument.

3.3 Indoor fate of the nitrate radical

As indicated in section 1, reactions of NO_3 with VOCs may lead to NO_x removal from the gas-phase, while reaction with NO leads to reformation of NO_2. Fig. 1 (panel d) suggests that the contribution of both reaction paths to L_{NO_3} varies. We thus define the fractional contribution F of NO_3 reactions with VOCs (represented by k^{NO_3}) to the overall NO_3 loss rate L_{NO_3}:

$$F = \frac{k^{NO_3}}{L_{NO_3}} = \frac{k^{NO_3}}{k^{NO_3} + k_3[NO]} \quad \text{(Eq. 5)}$$

The resulting fractional contributions are plotted together with measured (VOC-induced) NO_3 reactivities in Fig. 6. The mean fractional contribution of VOCs is 0.46 ± 0.31 (1σ). This implies that on average NO_3 was consumed roughly equally by NO and VOCs during the measurement period. It should be kept in mind that both the upper LOD of the k^{NO_3} measurement and the lower LOD of the NO measurement bias the calculated fractional contributions to higher values (potential overestimation of k^{NO_3} during NO-dominated periods and potential underestimation of NO-induced reactivity during VOC-dominated periods). During periods A–E, when N_2O_5 was above its LOD, the mean fractional contribution occasionally increased to 1, with a mean of 0.65 ± 0.32 (1σ). Both values are comparable to the nighttime outdoor values of 0.5–0.6 as observed at the summit of a semi-rural mountain site (impacted by both NO soil emissions and biogenic VOCs) *ca.* 30 km from the laboratory,[53] but lower than the values close to 1 as observed in forested regions where NO_3 reactivity is dominated by terpenes at night.[8,9] The closer agreement with nighttime

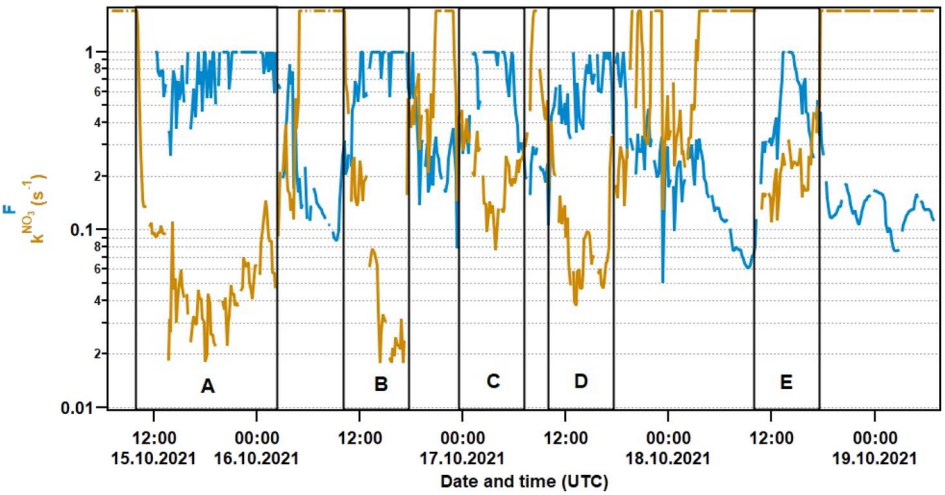

Fig. 6 NO_3 reactivity (k^{NO_3}) and fractional contribution F (Eq. 5) of k^{NO_3} to the overall NO_3 loss rate L_{NO_3}.

outdoor conditions in urban environments is easily understood considering the lack of NO_3 photolysis and the abundance of NO_x throughout the diel cycle. Moravek *et al.*[27] identified reaction with NO to be the dominant loss process in a highly-ventilated athletics facility during daytime, whereas the thermal equilibrium to N_2O_5 gained importance in the afternoon. Such a distinct diurnal variation is not observed in our short study.

Fig. 6 also shows that reaction with VOCs is a relevant NO_3 loss process most of the time in this particular environment. Unfortunately, there are no simultaneous VOC measurements available for this pilot study. Monoterpenes such as limonene are a class of organic compounds that are abundant in indoor environments due to their presence in detergents and cleaning agents[16,19,27] and which are highly reactive towards NO_3.[15] Terpenes or other unsaturated compounds released from indoor sources are thus the most likely organic reactants for NO_3. Reactive VOCs may however also originate from outside: the laboratory used in this study is located in the direct vicinity of deciduous trees, which at some times of the year can represent a significant source of isoprene as well as monoterpenes.[54–56] However, as our measurements were carried out in mid October with weak insolation and low temperatures, both of which result in low levels of biogenic activity, this is unlikely to represent the major source of indoor reactivity in this study.

4 Comparison to other indoor studies

In contrast to O_3 and OH, the nitrate radical has not been studied in indoor environments to a similar extent. Table 1 gives an overview of maximum mixing ratios of NO_3 (and N_2O_5) that were detected or modelled in different indoor environments.

As indicated in Fig. 1, up to 29 pptv of N_2O_5 were detected in our laboratory. The observation is comparable to 58 pptv of N_2O_5 + NO_3 (with N_2O_5 as the dominant fraction) that was observed inside an office building in Copenhagen, Denmark.[25] Note that both indoor environments were unoccupied, feature a comparable air change rate and are situated in urban areas. Arata *et al.*[26] reported 190 pptv of N_2O_5, if 40 ppbv O_3 was artificially added by a commercial ozone generator in order to force (together with 50–100 ppbv of NO_2) a very high NO_3 production rate of 7 ppbv h^{-1}. This is at least a factor of 10 higher than our

Table 1 Summary of studies on indoor measurements of NO_3 and N_2O_5[a]

Reference	Environment	Method	Max. NO_3/N_2O_5 (pptv)	Air change rate (h^{-1})
Carslaw[21]	Residential	Model calculation	0.03 (NO_3)	2
Nøjgaard[25]	Office (Copenhagen)	Indirect measurement	58 (NO_3 + N_2O_5)	3.76
Waring *et al.*[22]	Residential	Model calculation	0.07 (NO_3)	0.5
Zhou *et al.*[13]	Residential (New York)	Steady-state calculation	6.7×10^{-4} (NO_3)	0.65
Arata *et al.*[26]	Residential (Oakland)	CRDS	4 (NO_3)	1–1.4
Price *et al.*[23]	Museum (Boulder)	Steady-state calculation	0.04 (NO_3)	0.8
Moravek *et al.* [27]	Athletic facility (Boulder)	CIMS	4 (N_2O_5)	7
Link *et al.*[24]	Residential (Gaithersburg)	Model calculation	0.3 (NO_3)	0.24
This study	Laboratory (Mainz)	CRDS (N_2O_5)	29 (N_2O_5)	<4
		Steady-state calculation (NO_3)	6 (NO_3)	

[a] CRDS: Cavity ring-down spectroscopy, CIMS: chemical ionization mass spectrometry.

values of 0.04 to 0.2 pptv s^{-1} for P_{NO_3} and accounts for the lower N_2O_5 mixing ratios measured in our laboratory.

Recently, up to 4 pptv N_2O_5 (similar to our measurements in period C and E) were observed inside an athletics facility, which was not only more strongly ventilated (with an air change rate of 7 h^{-1}), but also occupied by humans.[27] In this case, NO_3 production rates between 0.025 and 0.3 pptv s^{-1} are similar to ours, so the lower maximum N_2O_5 mixing ratio is a reflection of higher NO_3 loss rates of up to 8 s^{-1} (at high-NO) compared to our median L_{NO_3} of 0.15 s^{-1}.

In a study by Price *et al.*,[23] oxidation *via* NO_3 contributes ~10% to the total VOC loss in a museum that is ventilated with an air change rate of only 0.8 h^{-1}. The dominant loss process in this museum is ventilation with the residual contribution of 90%. Despite the fact that our air change rate is higher by a factor of 5, we estimated a higher NO_3 contribution of ~30% (see above). This discrepancy is explained by different indoor NO_3 levels: According to steady-state calculations, only 0.04 pptv NO_3 were present in the museum which is two orders of magnitudes lower compared to our values.

Link *et al.*[24] identified ventilation to be the dominant VOC sink (88%) in a residential building featuring an even lower air change rate and modelled NO_3 level of 0.2 h^{-1} and 0.02 pptv, respectively. When 70 ppbv of O_3 were added artificially, oxidative processes competed with ventilation. In this case, ozonolysis (and OH production) drastically reduced the fractional contribution of (R7) to ~10%. Again, our higher fractional contribution of (R7) to the overall VOC loss is consequently reflected in our higher indoor NO_3 levels compared to those in Link *et al.*[24]

The NO_3 mixing ratios calculated from NO_2 and N_2O_5 mixing ratios (Fig. 1, panel e) are between 2 and 6 pptv and thus similar to the 3–4 pptv NO_3 that were directly measured in a residential kitchen[26] despite the great difference in P_{NO_3}. The comparable NO_3 levels are accordingly caused by the higher NO_3 reactivity of 0.8 s^{-1} (calculated from VOC measurements) in the residential kitchen. In any case, mixing ratios of a few pptv clearly exceed indoor NO_3 levels predicted in model or steady-state calculations for residential environments by a factor of ~100.[13,21–24] This underlines the necessity of more direct measurements of NO_3 mixing ratios, NO_3 reactivity, the traces gases responsible for the loss of NO_3 and also the products (*e.g.* organic nitrates) of indoor NO_3–VOC interactions.

5 Conclusions

We present the first direct NO_3 reactivity measurement in a ventilated indoor environment. Our pilot study suggests that the nitrate radical concentration increases, when (1) indoor air is continuously exchanged with outdoor air so that both O_3 and NO_2 are available, (2) NO is (almost) entirely depleted by O_3 and (3) the room is not directly exposed to sunlight. A high ventilation rate (~4 h^{-1}) resulted in a high correlation between indoor and outdoor mixing ratios of NO_2 and O_3. Measured N_2O_5 and calculated NO_3 mixing ratios peaked at 29 and 6 pptv, which are significantly higher than reported in model calculations[21,22] but which agree with observations made in other ventilated (non-residential) rooms.[25,27] We demonstrate that, in indoor environments when highly polluted conditions impede the formation of detectable amounts of NO_3, measuring the NO_3 reactivity simultaneously with NO_2 and O_3 represents an alternative way to assess NO_3 mixing ratios. Furthermore, our NO_3 measurements emphasized the necessity of frequent inlet filter changes as common in outdoor field measurements. By comparing calculated with directly measured NO_3 reactivities, we find that the most important loss processes for NO_3 are reactions with NO and VOCs (such as monoterpenes), the latter thus providing an indoor source of organic nitrates. Direct NO_3 reactivity measurements can therefore contribute to identify the indoor fate of the nitrate radical.

Author contributions

Patrick Dewald: conceptualization; data curation; formal analysis; investigation; methodology; visualization; writing – original draft; writing – review & editing. John N. Crowley: conceptualization; supervision; validation; writing – review & editing. Jos Lelieveld: resources; supervision; validation; writing – review & editing.

Conflicts of interest

There are no conflicts to declare.

Acknowledgements

We thank Chemours for provision of a FEP sample used to coat the flowtube reactor.

References

1 N. E. Klepeis, W. C. Nelson, W. R. Ott, J. P. Robinson, A. M. Tsang, P. Switzer, J. V. Behar, S. C. Hern and W. H. Engelmann, The National Human Activity Pattern Survey (NHAPS): a resource for assessing exposure to environmental pollutants, *J. Exposure Anal. Environ. Epidemiol.*, 2001, **11**, 231–252.

2 C. J. Weschler, M. Brauer and P. Koutrakis, Indoor Ozone and Nitrogen-Dioxide - a Potential Pathway to the Generation of Nitrate Radicals, Dinitrogen Pentaoxide, and Nitric-Acid Indoors, *Environ. Sci. Technol.*, 1992, **26**, 179–184.

3 C. J. Weschler and H. C. Shields, Production of the hydroxyl radical in indoor air, *Environ. Sci. Technol.*, 1996, **30**, 3250–3258.

4 C. J. Young, S. Zhou, J. A. Siegel and T. F. Kahan, Illuminating the dark side of indoor oxidants, *Environ. Sci.: Processes Impacts*, 2019, **21**, 1229–1239.

5 N. Zannoni, P. S. J. Lakey, Y. Won, M. Shiraiwa, D. Rim, C. J. Weschler, N. J. Wang, L. Ernle, M. Z. Li, G. Bekö, P. Wargocki and J. Williams, The human oxidation field, *Science*, 2022, **377**, 1071–1076.

6 R. P. Wayne, I. Barnes, P. Biggs, J. P. Burrows, C. E. Canosamas, J. Hjorth, G. Lebras, G. K. Moortgat, D. Perner, G. Poulet, G. Restelli and H. Sidebottom, The

Nitrate Radical - Physics, Chemistry, and the Atmosphere, *Atmos. Environ.*, 1991, **25**, 1–203.

7 S. S. Brown and J. Stutz, Nighttime radical observations and chemistry, *Chem. Soc. Rev.*, 2012, **41**, 6405–6447.

8 J. Liebmann, E. Karu, N. Sobanski, J. Schuladen, M. Ehn, S. Schallhart, L. Quéléver, H. Hellen, H. Hakola, T. Hoffmann, J. Williams, H. Fischer, J. Lelieveld and J. N. Crowley, Direct measurement of NO_3 radical reactivity in a boreal forest, *Atmos. Chem. Phys.*, 2018, **18**, 3799–3815.

9 J. M. Liebmann, J. B. A. Muller, D. Kubistin, A. Claude, R. Holla, C. Plaß-Dülmer, J. Lelieveld and J. N. Crowley, Direct measurements of NO_3-reactivity in and above the boundary layer of a mountain-top site: Identification of reactive trace gases and comparison with OH-reactivity, *Atmos. Chem. Phys.*, 2018, **18**, 12045–12059.

10 A. Gandolfo, V. Gligorovski, V. Bartolomei, S. Tlili, E. G. Alvarez, H. Wortham, J. Kleffmann and S. Gligorovski, Spectrally resolved actinic flux and photolysis frequencies of key species within an indoor environment, *Build. Environ.*, 2016, **109**, 50–57.

11 S. Zhou and T. F. Kahan, Spatiotemporal characterization of irradiance and photolysis rate constants of indoor gas-phase species in the UTest house during HOMEChem, *Indoor Air*, 2022, **32**, e12964.

12 C. J. Weschler, Ozone in indoor environments: Concentration and chemistry, *Indoor Air*, 2000, **10**, 269–288.

13 S. Zhou, C. J. Young, T. C. VandenBoer, S. F. Kowal and T. F. Kahan, Time-Resolved Measurements of Nitric Oxide, Nitrogen Dioxide, and Nitrous Acid in an Occupied New York Home, *Environ. Sci. Technol.*, 2018, **52**, 8355–8364.

14 W. W. Nazaroff and C. J. Weschler, Indoor ozone: Concentrations and influencing factors, *Indoor Air*, 2022, **32**, e12942.

15 N. L. Ng, S. S. Brown, A. T. Archibald, E. Atlas, R. C. Cohen, J. N. Crowley, D. A. Day, N. M. Donahue, J. L. Fry, H. Fuchs, R. J. Griffin, M. I. Guzman, H. Herrmann, A. Hodzic, Y. Iinuma, J. L. Jimenez, A. Kiendler-Scharr, B. H. Lee, D. J. Luecken, J. Mao, R. McLaren, A. Mutzel, H. D. Osthoff, B. Ouyang, B. Picquet-Varrault, U. Platt, H. O. T. Pye, Y. Rudich, R. H. Schwantes, M. Shiraiwa, J. Stutz, J. A. Thornton, A. Tilgner, B. J. Williams and R. A. Zaveri, Nitrate radicals and biogenic volatile organic compounds: oxidation, mechanisms, and organic aerosol, *Atmos. Chem. Phys.*, 2017, **17**, 2103–2162.

16 W. W. Nazaroff and C. J. Weschler, Cleaning products and air fresheners: exposure to primary and secondary air pollutants, *Atmos. Environ.*, 2004, **38**, 2841–2865.

17 N. L. Ng, A. J. Kwan, J. D. Surratt, A. W. H. Chan, P. S. Chhabra, A. Sorooshian, H. O. T. Pye, J. D. Crounse, P. O. Wennberg, R. C. Flagan and J. H. Seinfeld, Secondary organic aerosol (SOA) formation from reaction of isoprene with nitrate radicals (NO_3), *Atmos. Chem. Phys.*, 2008, **8**, 4117–4140.

18 J. L. Fry, A. Kiendler-Scharr, A. W. Rollins, T. Brauers, S. S. Brown, H. P. Dorn, W. P. Dube, H. Fuchs, A. Mensah, F. Rohrer, R. Tillmann, A. Wahner, P. J. Wooldridge and R. C. Cohen, SOA from limonene: role of NO_3 in its generation and degradation, *Atmos. Chem. Phys.*, 2011, **11**, 3879–3894.

19 G. Bekö, P. Wargocki, N. J. Wang, M. Z. Li, C. J. Weschler, G. Morrison, S. Langer, L. Ernle, D. Licina, S. Yang, N. Zannoni and J. Williams, The Indoor Chemical Human Emissions and Reactivity (ICHEAR) project: Overview of experimental methodology and preliminary results, *Indoor Air*, 2020, **30**, 1213–1228.

20 N. Carslaw, L. Fletcher, D. Heard, T. Ingham and H. Walker, Significant OH production under surface cleaning and air cleaning conditions: Impact on indoor air quality, *Indoor Air*, 2017, **27**, 1091–1100.

21 N. Carslaw, A new detailed chemical model for indoor air pollution, *Atmos. Environ.*, 2007, **41**, 1164–1179.

22 M. S. Waring and J. R. Wells, Volatile organic compound conversion by ozone, hydroxyl radicals, and nitrate radicals in residential indoor air: Magnitudes and impacts of oxidant sources, *Atmos. Environ.*, 2015, **106**, 382–391.

23 D. J. Price, D. A. Day, D. Pagonis, H. Stark, L. B. Algrim, A. V. Handschy, S. Liu, J. E. Krechmer, S. L. Miller, J. F. Hunter, J. A. de Gouw, P. J. Ziemann and J. L. Jimenez, Budgets of Organic Carbon Composition and Oxidation in Indoor Air, *Environ. Sci. Technol.*, 2019, **53**, 13053–13063.

24 M. F. Link, J. Li, J. C. Ditto, H. Huynh, J. Yu, S. M. Zimmerman, K. L. Rediger, A. Shore, J. P. D. Abbatt, L. A. Garofalo, D. K. Farmer and D. Poppendieck, Ventilation in a Residential Building Brings Outdoor NO_x Indoors with Limited Implications for VOC Oxidation from NO_3 Radicals, *Environ. Sci. Technol.*, 2023, **57**(43), 16446–16455.

25 J. K. Nøjgaard, Indoor measurements of the sum of the nitrate radical, NO_3, and nitrogen pentoxide, N_2O_5 in Denmark, *Chemosphere*, 2010, **79**, 898–904.

26 C. Arata, K. J. Zarzana, P. K. Misztal, Y. J. Liu, S. S. Brown, W. W. Nazaroff and A. H. Goldstein, Measurement of NO_3 and N_2O_5 in a Residential Kitchen, *Environ. Sci. Technol. Lett.*, 2018, **5**, 595–599.

27 A. Moravek, T. C. VandenBoer, Z. Finewax, D. Pagonis, B. A. Nault, W. L. Brown, D. A. Day, A. V. Handschy, H. Stark, P. Ziemann, J. L. Jimenez, J. A. de Gouw and C. J. Young, Reactive Chlorine Emissions from Cleaning and Reactive Nitrogen Chemistry in an Indoor Athletic Facility, *Environ. Sci. Technol.*, 2022, **56**, 15408–15416.

28 Y. Shah, J. W. Kurelek, S. D. Peterson and S. Yarusevych, Experimental investigation of indoor aerosol dispersion and accumulation in the context of COVID-19: Effects of masks and ventilation, *Phys. Fluids*, 2021, **33**, 073315.

29 R. A. Cox, M. Ammann, J. N. Crowley, P. T. Griffiths, H. Herrmann, E. H. Hoffmann, M. E. Jenkin, V. F. McNeill, A. Mellouki, C. J. Penkett, A. Tilgner and T. J. Wallington, Opinion: The germicidal effect of ambient air (open-air factor) revisited, *Atmos. Chem. Phys.*, 2021, **21**, 13011–13018.

30 M. H. Sherman, Tracer-Gas Techniques for Measuring Ventilation in a Single Zone, *Build. Environ.*, 1990, **25**, 365–374.

31 J. M. Liebmann, G. Schuster, J. B. Schuladen, N. Sobanski, J. Lelieveld and J. N. Crowley, Measurement of ambient NO_3 reactivity: Design, characterization and first deployment of a new instrument, *Atmos. Meas. Tech.*, 2017, **10**, 1241–1258.

32 N. Sobanski, J. Schuladen, G. Schuster, J. Lelieveld and J. N. Crowley, A five-channel cavity ring-down spectrometer for the detection of NO_2, NO_3, N_2O_5, total peroxy nitrates and total alkyl nitrates, *Atmos. Meas. Tech.*, 2016, **9**, 5103–5118.

33 N. Friedrich, I. Tadic, J. Schuladen, J. Brooks, E. Darbyshire, F. Drewnick, H. Fischer, J. Lelieveld and J. N. Crowley, Measurement of NOx and NOy with a thermal dissociation cavity ring-down spectrometer (TD-CRDS): instrument characterisation and first deployment, *Atmos. Meas. Tech.*, 2020, **13**, 5739–5761.

34 J. B. Burkholder, S. P. Sander, J. Abbatt, J. R. Barker, R. E. Huie, C. E. Kolb, M. J. Kurylo, V. L. Orkin, D. M. Wilmouth and P. H. Wine, *Chemical Kinetics and Photochemical Data for Use in Atmospheric Studies, Evaluation No. 18*, JPL Publication 15-10, Jet Propulsion Laboratory, Pasadena, **https://jpldataeval.jpl.nasa.gov**, accessed 23 July 2023.

35 IUPAC, *Task Group on Atmospheric Chemical Kinetic Data Evaluation*, ed. M. Ammann, R. A. Cox, J. N. Crowley, H. Herrmann, M. E. Jenkin, V. F. McNeill, A. Mellouki, M. J. Rossi, J. Troe and T. J. Wallington, **https://iupac.aeris-data.fr/en/home-english/**, accessed 23 July 2023.

36 M. J. Tang, J. Thieser, G. Schuster and J. N. Crowley, Uptake of NO_3 and N_2O_5 to Saharan dust, ambient urban aerosol and soot: a relative rate study, *Atmos. Chem. Phys.*, 2010, **10**, 2965–2974.

37 G. Schuster, I. Labazan and J. N. Crowley, A cavity ring down/cavity enhanced absorption device for measurement of ambient NO_3 and N_2O_5, *Atmos. Meas. Tech.*, 2009, **2**, 1–13.

38 *Umweltbundesamt*, **https://www.umweltbundesamt.de/en/data/air/air-data/**, accessed 12 June 2023.

39 Y. Hu and B. Zhao, Relationship between indoor and outdoor NO_2: A review, *Build. Environ.*, 2020, **180**, 106909.

40 T. Grontoft, The influence of photochemistry on outdoor to indoor NO_2 in some European museums, *Indoor Air*, 2022, **32**, e12999.

41 J. N. Crowley, G. Schuster, N. Pouvesle, U. Parchatka, H. Fischer, B. Bonn, H. Bingemer and J. Lelieveld, Nocturnal nitrogen oxides at a rural mountain site in south-western Germany, *Atmos. Chem. Phys.*, 2010, **10**, 2795–2812.

42 U. F. Platt, A. M. Winer, H. W. Biermann, R. Atkinson and J. N. Pitts, Measurement of Nitrate Radical Concentrations in Continental Air, *Environ. Sci. Technol.*, 1984, **18**, 365–369.

43 F. Heintz, U. Platt, H. Flentje and R. Dubois, Long-term observation of nitrate radicals at the tor station, Kap Arkona (Rügen), *J. Geophys. Res.: Atmos.*, 1996, **101**, 22891–22910.

44 M. Martinez, D. Perner, E. M. Hackenthal, S. Kulzer and L. Schutz, NO_3 at Helgoland during the NORDEX campaign in October 1996, *J. Geophys. Res.: Atmos.*, 2000, **105**, 22685–22695.

45 S. S. Brown, H. Stark, T. B. Ryerson, E. J. Williams, D. K. Nicks, M. Trainer, F. C. Fehsenfeld and A. R. Ravishankara, Nitrogen oxides in the nocturnal boundary layer: Simultaneous in situ measurements of NO_3, N_2O_5, NO_2, NO, and O_3, *J. Geophys. Res.: Atmos.*, 2003, **108**, 4299.

46 S. S. Brown, J. A. Degouw, C. Warneke, T. B. Ryerson, W. P. Dube, E. Atlas, R. J. Weber, R. E. Peltier, J. A. Neuman, J. M. Roberts, A. Swanson, F. Flocke, S. A. McKeen, J. Brioude, R. Sommariva, M. Trainer, F. C. Fehsenfeld and A. R. Ravishankara, Nocturnal isoprene oxidation over the Northeast United States in summer and its impact on reactive nitrogen partitioning and secondary organic aerosol, *Atmos. Chem. Phys.*, 2009, **9**, 3027–3042.

47 N. Sobanski, M. J. Tang, J. Thieser, G. Schuster, D. Pöhler, H. Fischer, W. Song, C. Sauvage, J. Williams, J. Fachinger, F. Berkes, P. Hoor, U. Platt, J. Lelieveld and J. N. Crowley, Chemical and meteorological influences on the lifetime of NO_3 at a semi-rural mountain site during PARADE, *Atmos. Chem. Phys.*, 2016, **16**, 4867–4883.

48 S. S. Brown, H. Stark and A. R. Ravishankara, Applicability of the steady state approximation to the interpretation of atmospheric observations of NO_3 and N_2O_5, *J. Geophys. Res.: Atmos.*, 2003, **108**, 4539.

49 P. Dewald, J. M. Liebmann, N. Friedrich, J. Shenolikar, J. Schuladen, F. Rohrer, D. Reimer, R. Tillmann, A. Novelli, C. M. Cho, K. M. Xu, R. Holzinger, F. Bernard, L. Zhou, W. Mellouki, S. S. Brown, H. Fuchs, J. Lelieveld and J. N. Crowley, Evolution of NO_3 reactivity during the oxidation of isoprene, *Atmos. Chem. Phys.*, 2020, **20**, 10459–10475.

50 C. J. Weschler and H. C. Shields, Measurements of the hydroxyl radical in a manipulated but realistic indoor environment, *Environ. Sci. Technol.*, 1997, **31**, 3719–3722.

51 N. Carslaw, A mechanistic study of limonene oxidation products and pathways following cleaning activities, *Atmos. Environ.*, 2013, **80**, 507–513.

52 T. H. Bertram and J. A. Thornton, Toward a general parameterization of N_2O_5 reactivity on aqueous particles: the competing effects of particle liquid water, nitrate and chloride, *Atmos. Chem. Phys.*, 2009, **9**, 8351–8363.

53 P. Dewald, C. M. Nussbaumer, J. Schuladen, A. Ringsdorf, A. Edtbauer, H. Fischer, J. Williams, J. Lelieveld and J. N. Crowley, Fate of the nitrate radical at the summit of a semi-rural mountain site in Germany assessed with direct reactivity measurements, *Atmos. Chem. Phys.*, 2022, **22**, 7051–7069.

54 C. Calfapietra, S. Fares, F. Manes, A. Morani, G. Sgrigna and F. Loreto, Role of Biogenic Volatile Organic Compounds (BVOC) emitted by urban trees on ozone concentration in cities: A review, *Environ. Pollut.*, 2013, **183**, 71–80.

55 E. C. Lahr, G. W. Schade, C. C. Crossett and M. R. Watson, Photosynthesis and isoprene emission from trees along an

urban–rural gradient in Texas, *Global Change Biol.*, 2015, **21**, 4221–4236.
56 Y. Gao, M. Ma, F. Yan, H. Su, S. Wang, H. Liao, B. Zhao, X. Wang, Y. Sun, J. R. Hopkins, Q. Chen, P. Fu, A. C. Lewis, Q. Qiu, X. Yao and H. Gao, Impacts of biogenic emissions from urban landscapes on summer ozone and secondary organic aerosol formation in megacities, *Sci. Total Environ.*, 2022, **814**, 152654.
57 D. York, Least-Squares Fitting of a Straight Line, *Can. J. Phys.*, 1966, **44**, 1079–1086.